

M.O. SHABANI\*, A. MAZAHERY\*

## COMPUTATIONAL FLUID DYNAMICS (CFD) SIMULATION OF LIQUID-LIQUID MIXING IN MIXER SETTLER

### ZASTOSOWANIE OBLICZENIOWEJ MECHANIKI PŁYNÓW DO SYMULACJI MIESZANIA CIECZ-CIECZ W EKSTRAKTORZE

Mixer-settlers are widely used in metallurgical, mineral and chemical process. One of the greatest challenges in the area of hydrometallurgy process simulation is agitation made by impeller inside mixer-settler which yet presents one of the most common operations. Computational fluid dynamics (CFD) model has been developed to predict the effect of different physical parameters including temperature and density on the mixing characteristics of the system. It is noted that non-isotropic nature of flow in a mixer-settler, the complex geometry of rotating impellers and the large disparity in geometric scales present are some of the factors which contribute to the simulation difficulty. The experimental data for different velocity outlet was also used in order to validate the model.

*Keywords:* Mixer-settler, CFD, Mixing

Mieszanie w ekstraktorze (mieszalniku-odstojniku) jest jedną z najczęstszych operacji, ale stanowi jedno z największych wyzwań dla symulacji komputerowej. Ekstraktory zazwyczaj zawierają wirnik zamontowany na wale, i ewentualnie mogą zawierać przegrody. W niniejszej pracy badano właściwości hydrodynamiczne ekstraktorów. Zbadano wpływ różnych parametrów fizycznych, temperatur i gęstości, na mieszanie w układzie. Model oparty na obliczeniowej mechanice płynów (Computational Fluid Dynamics) został opracowany w celu przewidywania charakterystyki mieszania. Model został zweryfikowany za pomocą danych doświadczalnych dla różnych szybkości stosowanych w pracy. Praca pozwoliła na zwiększenie efektywności ekstraktorów, które mogą charakteryzować się wyższymi parametrami niż te podawane w literaturze.

## 1. Introduction

Mixer-settlers are widely used in metallurgical, mineral and chemical process such as: petroleum industry, water industry, hydrometallurgy, biotechnology, food industry, waste management, etc. Study of turbulent flow and computation of its properties in a mixer-settler is a considerable challenge for existing turbulence models. Factors contributing to this difficulty include the non-isotropic nature of flow in a mixer-settler, the complex geometry of rotating impellers and the large disparity in geometric scales present. Existence of baffles also increases the complexity of the flow field. Analyzing the turbulent flow pattern and its properties in mixer-settler may be a beneficial tool for equipment design, process scale-up, energy conservation and product quality control [1-6].

The function of the mixer is to provide an adequate combination of mixing and dispersion for the desired degree of extraction. When the impeller rotates, a low

pressure region is developed in the vicinity of the impeller. This low pressure region causes mixing of the phases into the mixer [7-11]. A large number of CFD simulations have been carried out in this study. The objectives of the present work are as follows: Investigate the effect of different temperature, viscosity and density.

## 2. Experimental

A side view and top view of the mixer-settler is shown in Fig. 1 that has been constructed from plexiglass for laboratory experimental purpose. Two inlets are located down of the impeller. The mixer is equipped with four baffles that generated dispersion overflows into the gravity settler for phase separation. The impeller axis was centrally located in the mixer-settler 10 mm from the inlets and mixer bottom. The vertical position of the impeller could be altered, if desired, by changing impeller shafts. The speed could be varied between 0 and 300 rpm by means of a motor controller equipped with a display.

\* HASHTGERD BRANCH, ISLAMIC AZAD UNIVERSITY, HASHTGERD, IRAN

The liquid is pumped into the feed tanks at a known inlet velocity (pump model: ISMATEC, TSM831C).

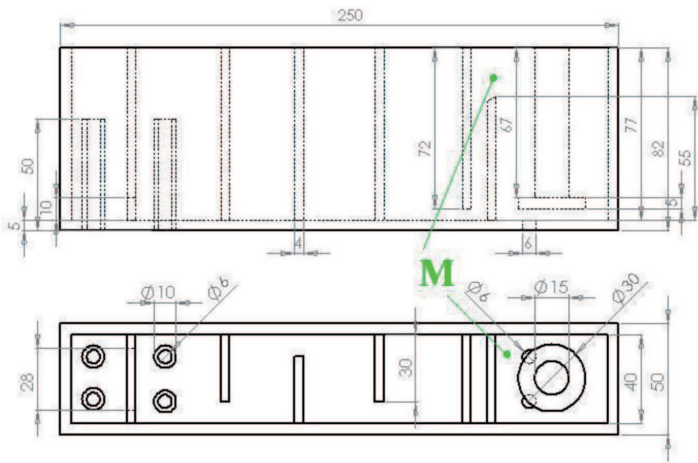


Fig. 1. Scale drawing for mixer-settler

### 3. CFD simulations

CFD simulations involve solution of discretized equations continuity equation for incompressible flow and time averaged Navier–Stokes equations:

Continuity:

$$\nabla \cdot \rho \vec{v} = 0 \quad (1)$$

Where  $\rho$  is the density and  $\vec{v}$  is the velocity vector.

Momentum balance:

$$\nabla \cdot \rho \vec{v} \vec{v} = -\nabla P + (\nabla \cdot \vec{\tau}) + \rho g + \vec{F} \quad (2)$$

Where  $\vec{\tau}$  is the stress tensor expressed as:

$$\vec{\tau} = \mu [(\nabla \vec{v} + (\nabla \vec{v})^T) - \frac{2}{3} \nabla \cdot \vec{v}] \quad (3)$$

And  $g, P, \mu$  and  $\vec{F}$  are the gravitational force, pressure, dynamic viscosity and external force respectively [11].

Turbulent mixing layers are commonly observed in various engineering applications such as combustion and environmental flows. The  $k$ - $\varepsilon$  model is one of a family of two-equation models, for which two additional transport equations must be solved in order to compute the Reynolds stresses. It is applicable to a wide variety of turbulent flows, and has served the fluid modeling community for many years. The two transport equations that need to be solved for this model are for the kinetic energy of turbulence ( $k$ ), and the rate of dissipation of turbulence ( $\varepsilon$ ) [12, 13]. The hypothesis also introduces another term involving a new variable,  $k$ , and the kinetic energy of turbulence. This quantity is defined in terms

of the velocity fluctuations  $u, v,$  and  $w$  in each of the three coordinate directions:

$$k = \frac{1}{2}(\bar{u}^2 + \bar{v}^2 + \bar{w}^2) \quad (4)$$

$$\frac{\delta(\rho k)}{\delta t} + \frac{\delta}{\delta x_i}(\rho U_i k) = \frac{\delta}{\delta x_i}(\mu + \frac{\mu_t}{\sigma_k}) \frac{\delta k}{\delta x_i} + G_k - \rho \varepsilon \quad (5)$$

$$\frac{\delta(\rho \varepsilon)}{\delta t} + \frac{\delta}{\delta x_i}(\rho U_i \varepsilon) = \frac{\delta}{\delta x_i}(\mu + \frac{\mu_t}{\sigma_\varepsilon}) \frac{\delta \varepsilon}{\delta x_i} + C_1 \frac{\varepsilon}{k} G_k + C_2 \rho \frac{\varepsilon^2}{k} \quad (6)$$

The quantities  $C_1, C_2, \sigma_k$  and  $\sigma_\varepsilon$  are 1.44, 1.92, 1.00 and 1.30 respectively. The quantity  $G_k$  appearing in both equations is a generation term for turbulence. It contains products of velocity gradients, and also depends on the turbulent viscosity where  $\rho$  is the fluid density,  $U$  is the mean velocity vector and  $\mu$  is the molecular or dynamic viscosity of the fluid. The new constant,  $\mu_t$ , is the turbulent, or eddy viscosity [11].

$$G_k = \mu_t \left( \frac{\delta U_i}{\delta x_j} + \frac{\delta U_j}{\delta x_i} \right) \frac{\delta U_j}{\delta x_i} \quad (7)$$

$$\mu_t = \rho C_\mu \frac{k^2}{\varepsilon} \quad (8)$$

#### 3.1. Computational grids

The geometry of the mixer settler was modeled in GAMBIT. The flow in the complex channel which is studied in this paper is inherently three-dimensional. A 2D simulation cannot pick up the fluid flows in the third direction and this can result in a lower accuracy of the numerical predictions. In 3D simulations, the baffles, impellers, and other internals can be modeled using their exact geometry. Therefore, in this paper a full 3D flow simulation has been employed.

Although Fluent is basically able to treat structural mesh type, the numerical solver of it did not reach any convergence. Therefore, a completely unstructured grid was generated which was optimized for its performance with approximately 0.8 million cells. This nodalization includes every flow-relevant detail and abstains from simplifications. Furthermore, hexahedral cells have been applied for meshing model.

#### 3.2. Boundary conditions

At the inlet, a constant flow rate was specified and at the outflow of the mixing channel, pressure outlet boundary condition was assumed. The momentum reflection back into the computational domain was assumed to be normal to the outlet. Turbulence of the fluid back into the computational domain was specified approximately by the turbulent intensity and hydraulic diameter of the

flow channel. No velocity slip exists at solid walls and the standard wall functions are used for near-wall treatment. A velocity magnitude is set at the inlet and zero gauge pressure is set at the outlet.

### 3.3. Solver

Fluid motion is calculated by directly solving the Navier Stokes equations. Second order discretization scheme is used for momentum, turbulent kinetic energy and for the energy dissipation. Commercial CFD software, Fluent 6.3 was used to simulate the flow fields under different operating conditions. SIMPLE (Semi-Implicit Method to solve Pressure Linked Equations) method was used for the pressure–velocity coupling. SIMPLE determines the pressure field indirectly by closing the discretised momentum equations with the continuity equations in a sequential manner. A 3D, segregated, implicit, steady solver algorithm was used for predicting the velocity and turbulence fields. Then  $k-\epsilon$  turbulence model was defined. Under relaxation factors, 0.3, 1.0, 1.0, 0.7, 0.8, and 0.8 were chosen for pressure, density, body forces, momentum, kinetic energy, and dissipation, respectively. During the solution for mixing, solutions for the flow field were held constant [13, 14].

The method to judge convergence was to monitor the magnitude of scaled residuals. Residuals are defined

as the imbalance in each conservation equation following each iteration. The convergence criteria was set that the governing equations are iteratively solved until at all nodes in the computational domain the relative changes in pressure and velocity components between two successive iterations become less than  $10^{-6}$  (residual monitors).

### 4. Results

A total of 20 final CFD runs were carried out representing different combinations of variables like temperatures, viscosity and density. Figure 2 shows velocity vectors colored by volume fraction for phase 1 and Figure 3 shows path lines colored by volume fraction for phase 1. In the mixing process of the primary and secondary fluid, the momentum of the two fluids is exchanged through the flow layer. The function of the mixer is to provide an adequate combination of mixing and dispersion for the desired degree of extraction. For optimized condition in mixer settler we must find minimum consuming power in maximum amount of mixing. In point M, if we consider that the inlet velocity is equal for two phases the optimal condition is obtained when power consumption is minimum and volume fraction is 0.5.

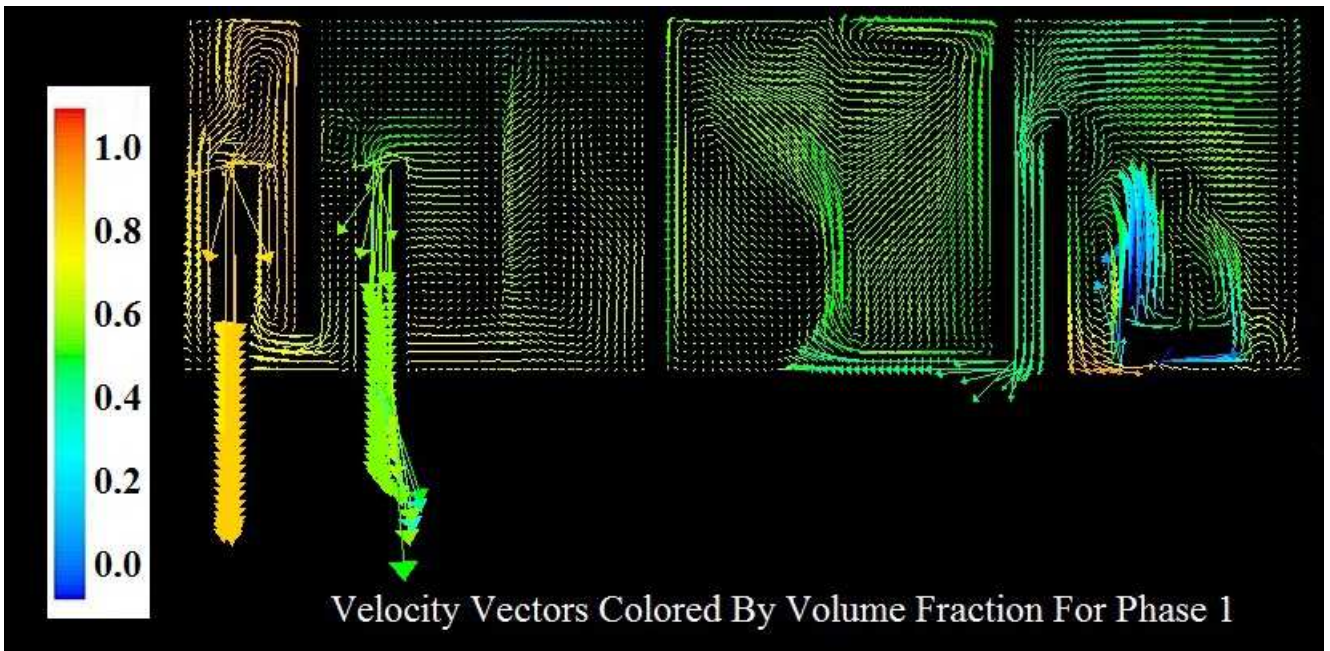


Fig. 2. Velocity vectors colored by volume fraction for phase 1

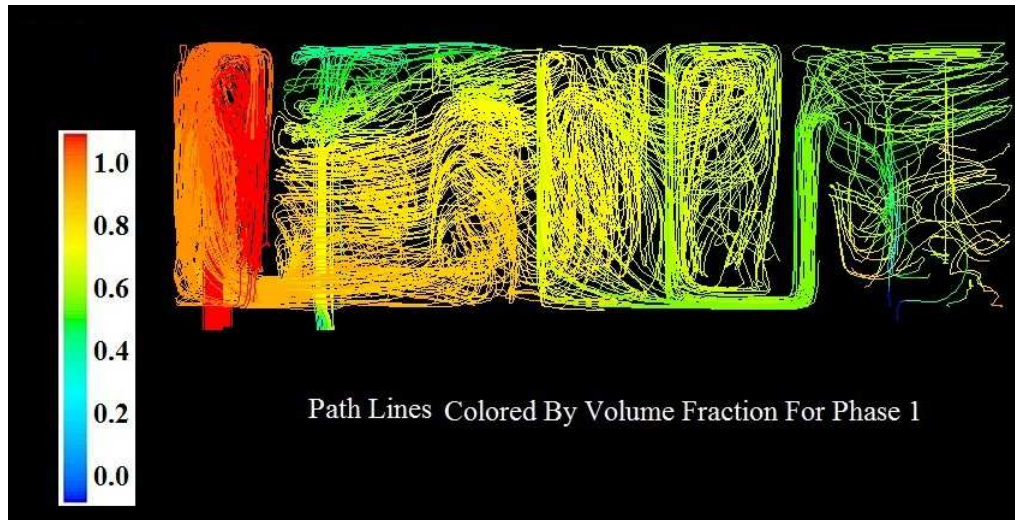


Fig. 3. Path lines colored by volume fraction for phase 1

#### 4.1. Effect of density

When multiple fluids are involved in a flow field, representing them by multiple species equations only works if the fluids are mixing and not separating. Any separation caused by the action of body forces, such as centrifugal force or gravity, can only be captured by treating the fluids with a multiphase model. When such a model is used, each of the fluids is assigned a separate set of properties, including density. Since different densities are used, forces of different magnitude can act on the fluids, enabling the prediction of separation. Figure 4 shows amount of mixing percentage as a function of impeller speed for inlet velocity of 0.1 (m/Sec) in  $\Delta\rho$  10%, 25% and 40%. CFD modelling approaches show that power consumption by the impeller is hardly affected

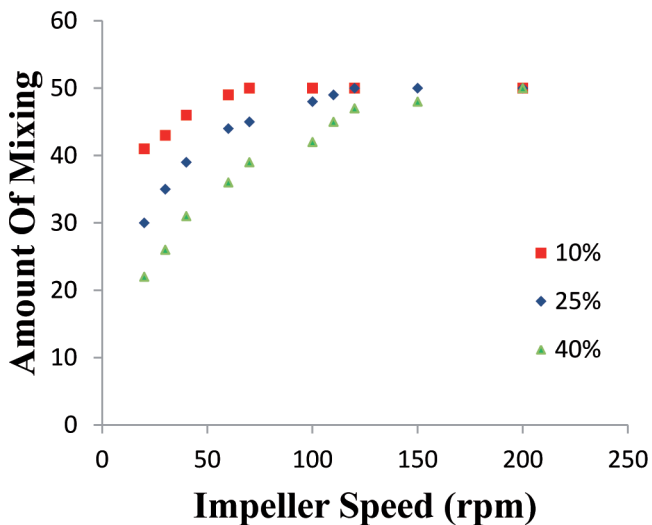


Fig. 4. Amount of mixing percentage as a function of impeller speed and density

by density. In the mixing process the momentum of the two fluids is exchanged through the flow layer. When difference between densities of two liquids is decreased condition for mixing is better and we could obtain better mixing in constant impeller speed. But when difference between two densities is less than 0.1, there is not enough time for separation phases; increased mixing intensity can produce a dispersion which is more difficult to separate, resulting in greater settler size requirements and higher entrainment levels.

#### 4.2. Effect of temperature and viscosities

Temperature is an important parameter in settler design. A rule of thumb states that a 20°C temperature increase can typically result in a doubling of settler capacity. The increase in settler capacity with temperature can be attributed to a decrease in liquid viscosities. Decreased viscosities result in higher coalescence rates due to easier drainage of the continuous phase film trapped between the droplets. Also, with respect to the separation mechanism proposed by previous work, the decrease in continuous phase viscosity would result in a smaller critical droplet size. The equilibrium between mechanical shearing and re-coalescence in the mixer could also be affected so as to produce a dispersion of a greater or lesser average drop size. Because of the appreciable effect of temperature, a mixer-settler test unit should include a temperature control system. In Fig. 5, shows that a higher operating temperature results in an increased efficiency. This can be attributed primarily to the decrease in the continuous phase viscosity with increased temperature which does the following [15]:

- Increases the rate of drainage of the continuous phase between 2 drops, facilitating more rapid coalescence.

- Increases the terminal settling velocity of the droplets.

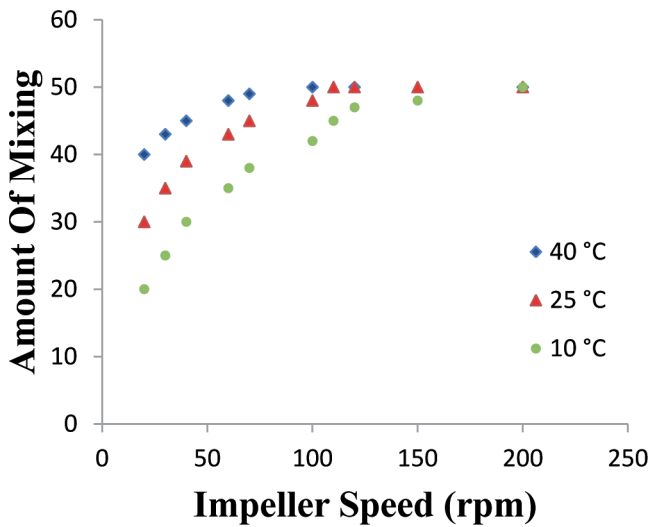


Fig. 5. Amount of mixing percentage as a function of impeller speed and temperature

Figure 5 shows amount of mixing percentage as a function of impeller speed and temperature for inlet velocity of 0.1 (m/Sec) in 10, 25 and 40°C. CFD data show that the amount of mixing increase with increasing tem-

perature. This is obvious, because in the mixing process of the primary and secondary fluid, the momentum of the two fluids is exchanged through the flow layer and when temperature increased, viscosity decreased and condition for mixing improved. But when temperature more than 40°C, there is no enough time for separation phases, increased mixing intensity can produce a dispersion which is more difficult to separate, resulting in greater settler size requirements and higher entrainment levels. Figure 6 shows contour of volume fraction for phases for mixer-settler that obtained from CFD (Temperature = 25°C,  $\Delta\rho = 25\%$ , impeller speed = 100 rpm and inlet velocity = 0.1 m/Sec).

### 5. Validation

Validation is a necessary part of the modelling process and the yardstick of success is the level of agreement that can be attained between numerical predictions and experiments. In this research outlet velocity between simulation and experimental are compared. Figure 7 shows outlet velocity as a function of total flow rate (Q) for experimental and simulation. It can be seen outlet velocity in experimental and simulation are close.

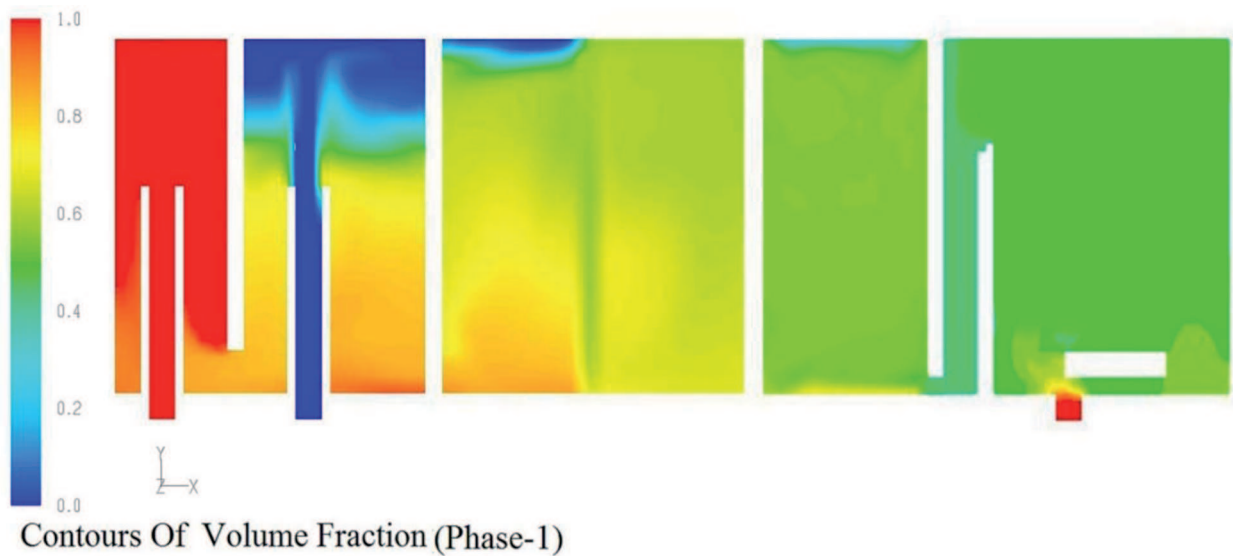


Fig. 6. Contour of volume fraction for phase-1

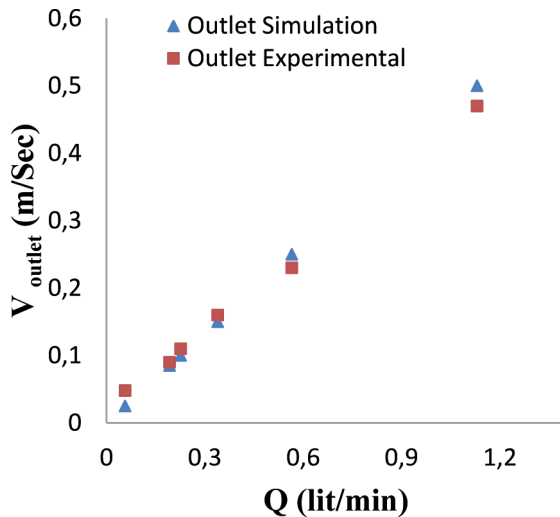


Fig. 7. Outlet velocity as a function of total flow rate

## 6. Conclusion

It is concluded that the analysis of the turbulent flow pattern and its properties in mixer-settler may be a beneficial tool for equipment design, process scale-up, energy conservation and product quality control. The result shows that the existence of baffles increases the complexity of the flow field. Regarding the mixing intensity, it is shown that extraction efficiencies can be improved by increasing the intensity. However, consideration must also be given to the possible effects that they may have on the phase separation process. In industrial operation, the increased settler capacity facilitated by operation at higher temperatures must be weighed against any extra costs associated with heating of process solutions. This work has enabled developing efficiency that can produce

better conditions than those reported in the previous literature.

## REFERENCES

- [1] M.H. Vakili, M.Esfahany, CES 64, 351-362 (2009).
- [2] E.F. Gomes, M.M.L. Guimaraes, L.M. Ribeiro, Advances in Engineering Software 38, 810-817 (2007).
- [3] K. Takahashi, A. Abdel, S.A. Tawab, T. Yajima, F. Kawaizumi, CES 57, 469-478 (2002).
- [4] Y.N. Chiu, J. Naser, K.F. Ngian, K.C. Pratt, ECM 48, 2556-2564 (2007).
- [5] H.D. Zughbi, M.A. Rakib, CES 59, 829-842 (2004).
- [6] R.N. Reeve, J.C. Godfry, Trans IChemE 80, Part A, November 2002.
- [7] M.T. Mostaedi, J. Safdari, M.A. Moosavian, M.G. Maragheh, CEP 48, 1249-1254 (2009).
- [8] K. Pianthong, W. Seehanam, M. Behnia, T. Sriveerakul, ECM 48, 2556-2564 (2007).
- [9] R.N. Meroney, P.E. Colorado, water research 43, 1040-1050 (2009).
- [10] C. Srilatha, Tushar P. Mundada, A.W. Patwardhan, ECRM 88, 10-22 (2010).
- [11] Binxin Wu, water research 1-13 (2009).
- [12] B.N. Murthy, J.B. Joshi, CES 63, 5468-5495 (2008).
- [13] K.K. Singh, K.T. Shenoy, A.K. Mahendra, S.K. Ghosh, CES 59, 2937-2945 (2004).
- [14] K.K. Singh, S.M. Mahajani, K.T. Shenoy, A.W. Patwardhan, S.K. Ghosh, CES 62, 1308-1322 (2007).
- [15] L. Eckert, B.A. Sc, The University of British Columbia 1984.